Accelerator mode in a gravitational bouncer as an attracting mode in a globally chaotic Hamiltonian system

S. T. Dembiński and P. Pepłowski
Institute of Physics, Nicholas Copernicus University, ulica Grudziądzka 5, 87-100 Toruń, Poland
(Received 27 June 1996)

An accelerator mode in a gravitational bouncer is studied. It is shown that this mode plays the role of a sink that eventually sucks out all of the diffusive component of the motion. In order to quantitatively describe this feature, a Fokker-Planck equation for the density P_D of the probability distribution of the diffusive mode is analytically transformed into a system of coupled Volterra-type integral equations that are subsequently numerically solved. A formula for the probability distribution P_{ACC} in the accelerator mode is also given. Numerical simulations reveal very satisfactory agreement with the proposed formulas. [S1063-651X(97)06801-3]

PACS number(s): 05.45.+b, 03.20.+i

I. INTRODUCTION

It is well known that when the dynamics of a nonlinear Hamiltonian system can be described in a two-dimensional phase space the chaotic part of the evolution is ruled by a Fokker-Planck equation for the distribution of one of the two variables. This variable is customarily taken to be the action I (or energy) and it is assumed that the other variable (angle) randomizes much more rapidly.

Two-dimensional mappings were the most frequently studied models of such systems (in this case action and angle are often replaced by momentum p and phase) and the central problem was connected to the determination of the diffusion coefficient $D(p)$. For the double periodic standard map the diffusion coefficient was calculated, taking into account long-time correlation effects, i.e., going beyond the quasilinear approximation, which assumes phase randomization on each mapping iteration [1,2]. It was shown that this result may be applied to more generic maps, e.g., the Fermi map, for which the standard map may be considered as a local approximation [7].

It soon became clear that the influence of a class of important phenomena that are present in a standard map was still missing in such a description of diffusion. These phenomena, called accelerator modes, were introduced by Chirikov [3]. In brief, in the chaotic sea of the phase space, there are islands of such regular motions for which the central trajectory has a constant phase while momentum p increases monotonically in time (within such an island phases perform a stable oscillation around the central fixed value). Accelerated motions of this type, called an accelerator mode, are classified according to their periodicity p and the step size l [4] and each type is stable within some interval of the parameter K characteristic for the standard map. No stochastic trajectory can enter a stable accelerator mode and there are no trajectories that can leave the mode either. In other words, the probabilities of finding a particle in the diffusive mode or a stable regular mode are time independent, i.e., at any instant of time they are the same as they were in the initial ensemble. However, even in the case when no orbits had initial phase-space coordinates lying within a stable accelerator-mode island, the enhancement of diffusion was observed. It is due to the intermittent transition of particles from the chaotic orbits to the unstable accelerator orbits, i.e., trajectories lying close to the accelerator islands. These trajectories will follow the stable accelerator orbits for many mapping periods and this effect is sometimes called ''the stickiness'' of islands [5].

More general mappings in which K is p dependent may not have stable accelerator modes. Even in this case, however, the enhancement of diffusion is expected because of the presence of the so-called latent accelerator modes or quasi-accelerator modes [6,7]. In some channels of the phase space, acceleration from p_0 to p_1 may occur if in the standard map the birth at $K(p_0)$ and the death at $K(p_1)$ of the accelerator mode respectively take place. Streaming over the mode was described in [7] by adding sources and sinks to the Fokker-Planck equation. This procedure would not be necessary if the integration time was long enough to include the entire period of streaming. In the type of maps considered there was also no net escape of probability from the diffusive mode.

Adding noise to the standard map ensures that every trajectory visits the stable accelerator modes for some time and modification of the diffusion takes place too. The dependence of this effect on the stochasticity parameter was investigated in [6].

The escape of the probability from the accelerator mode was proposed in [8]. In this paper the quantization of the kicked-rotator Hamiltonian, which corresponds to the standard map, was performed and the effect of the tunneling from the accelerator mode was taken into account. In particular, the dependence of the effect on the magnitude of the Planck constant was investigated.

The aim of the present paper is to introduce and analyze a physically well founded model that exhibits a number of features concerning the behavior and coexistence of diffusive and accelerator modes. It seems that the most important is the appearance of a type of the accelerator mode that acts as a sink for the diffusive mode and eventually sucks out all of the diffusive mode. Since it does happen irrespectively of the initial conditions, such a tendency for any diffusive motion

to become a motion within the accelerator mode resembles, in this respect only, tending towards motions on attractors in dissipative systems. The definition of the model will be followed by the description of its fundamental acceleration mode. Then, the Fokker-Planck equation for the density of the conditional probability for the diffusive mode will be solved exactly. Next, the solution of the equation for the diffusive probability density that includes sinks resulting from the accelerator mode will be presented. The numerical solution of the Volterra-type coupled integral equation will be used for the description of the sinks efficiency. Formulas for the probability density to find the trajectories in the accelerator mode are simultaneously derived and in this case the diffusion mode will be treated as a source. The formalism ensures the conservation of the sum of probabilities to find a trajectory in the diffusive or the accelerator mode. A comparison with numerical simulation will demonstrate that the theoretical description of the model proposed is generally correct.

II. MODEL

We are considering here the one-dimensional gravitational bouncer, i.e., a point mass m in the potential $U(x)$: $U(x)=mgx$ for $x>\varepsilon l(t)$ and $U(x)=\infty$ for $x\leqslant\varepsilon l(t)$. The function $l(t)$ is a real-valued periodic function (with period 1) of the dimensionless time parameter t and ε is a real positive parameter. An extensive bibliography on this model may be found in [9]. It will be assumed hereafter that $l(t)$ has the form

$$l(t)=\begin{cases} l_1(\{t\})/4g & \text{for } \xi\geqslant\{t\}\geqslant 0 \\ l_2(\{t\})/4g & \text{for } 1\geqslant\{t\}\geqslant\xi, \end{cases} \tag{1}$$

where $l_1(t)=-t(t-\xi)/\xi$, $l_2(t)=(t-\xi)(t-1)/(1-\xi)$, $\{t\}=t \bmod 1$, ξ is a real parameter, and $1\geqslant\xi\geqslant 0$. The above choice of $l(t)$ is not essential for investigations presented in the present paper; similar effects may be obtained for other forms of $l(t)$, e.g., $l(t)=\sin(2\pi t)$. Assuming the collisions at $x=l(t)$ to be elastic, setting $m=1$, and introducing the variable $p=2v/g$ (v is the point velocity), the dynamics of the bouncing ball is given by the map

$$\begin{aligned} p_{n+1}&=p_n+\varepsilon\dot{l}(t_{n+1})-\varepsilon[l(t_{n+1})-l(t_n)]/(t_{n+1}-t_n), \\ t_{n+1}&=t_n+p_n-\varepsilon[l(t_{n+1})-l(t_n)]/2(t_{n+1}-t_n), \end{aligned} \tag{2}$$

where t_n is the time of the nth collision, p_n is the scaled momentum just after the nth collision, and $\dot{l}$ denotes the derivative of l with respect to t. The map given in Eq. (2) will be called the ''collision map'' (CM).

Three linearly stable regular solutions of the CM can be easily found: (i) the periodic resonance solution $t_n^{(e)}=\xi/2$, $p_n^{(e)}=m$ with $m=1,2,\ldots$, $(t_{n+1}^{(e)}-t_n^{(e)}=m)$, which is stable for $0\leqslant\varepsilon\leqslant 2\xi$; (ii) the accelerator solution $t_n^{(a)}=\xi(1-1/\varepsilon)/2$, $p_n^{(a)}=N+n$, $n=0,1,2,\ldots$, $N=1,2,\ldots$, $(t_{n+1}^{(a)}-t_n^{(a)}=N+n)$, which is stable for $1\leqslant\varepsilon\leqslant 2\xi$ provided $\xi\geqslant 0.5$; and (iii) the deaccelerator solution $t_n^{(d)}=\xi(1+1/\varepsilon)/2$, $p_n^{(d)}=N-n$, $n=0,1,\ldots,N-1$, $N=2,3,\ldots$, $(t_{n+1}^{(d)}-t^{(d)_n}=N-n)$, in which the conditions for linear stability are the same as those for case (ii).

Points $(t_n^{(\,)},p_n^{(\,)})$ that belong to one of the above solutions represent the central trajectory in a bundle of neighboring trajectories describing similar regular motions of the bouncer. Numerical simulations reveal that global chaos appears in the CM for $\varepsilon\approx 1$. Then, on the (t_n,p_n) plane the bundles are viewed as islands of regular motion embedded in the sea of chaotic motion. They will be called resonance or the ''elliptic mode'' (EM), the ''accelerator mode'' (AM), and the ''deaccelerator mode'' (DAM) for cases (i), (ii), and (iii), respectively. The chaotic motion will be called the ''diffusive mode'' (DM).

The CM is not the area-preserving map. In fact,

$$\begin{aligned} &dp_{n+1}dt_{n+1} \\ &\quad=\left|[p_n-\varepsilon\dot{l}(t_n)/2]/[p_{n+1}-\varepsilon\dot{l}(t_{n+1})/2]\right|dp_n dt_n . \end{aligned} \tag{3}$$

On central trajectories, the above Jacobi determinant equals 1 for the EM, is smaller than 1 for the AM, and is greater than 1 for the DAM.

It can be seen from Eqs. (2) that for sufficiently large values of p_n the term $\varepsilon\left|[l(t_{n+1})-l(t_n)]/(t_{n+1}-t_n)\right|\ll 1$. Without this term the CM becomes very similar to the famous standard map in its particular form, which is called a piecewise linear standard map [12]. This approximate form of the CM will be further denoted as ACM. The ACM preserves area for each point (t_n,p_n), has the same three regular solutions as the CM (for m and $N\gg 1$), and the stability conditions are formally also the same. Let us stress at this point that apart from this asymptotic region, the CM cannot be locally approximated by a standard type of map even with ε depending on p_n. Such an approximation proved to be very useful in the case of the Fermi map [7].

Further studies will be performed on another, more convenient, form of the map that describes the dynamics of the bouncer in its phase space. The map, which will be called the ''stroboscopic map'' (SM), gives the values of position x and momentum v at consecutive integer instants of time $\tau=k$, $k=1,2,\ldots$.

Relations between (p_n,t_n) from the CM and (x,v) from the SM, taken at time τ, have the form

$$\begin{aligned} x&=-(g/2)(\tau-t_n)^2+gp_n(\tau-t_n)/2+l(t_n), \\ v&=-g(\tau-t_n)+gp_n/2. \end{aligned} \tag{4}$$

The point (p_n,t_n) generates $M=\mathrm{int}(p_n)$ points (x,v) whose values are obtained when $\tau=1,2,\ldots,M$ is substituted into Eq. (4).

Note that

$$dv\,dx|_\tau=(g/2)^2\left|[p_n-\varepsilon\dot{l}(t_n)/2]\right|dp_n dt_n \tag{5}$$

and observe that the Jacobi determinant is τ independent. Equations (3) and (5) confirm the area-preserving property of the SM.

In Fig. 1 a segment of the phase space of the SM is presented. Three regular solutions are clearly visible. Large elliptic areas represent islands of the EM. Families of islands that correspond to $p_n^{(e)}=1$, 2, and 3 are visible. The brightest areas represent islands of the AM, while the darkest ones depict islands of the DAM.

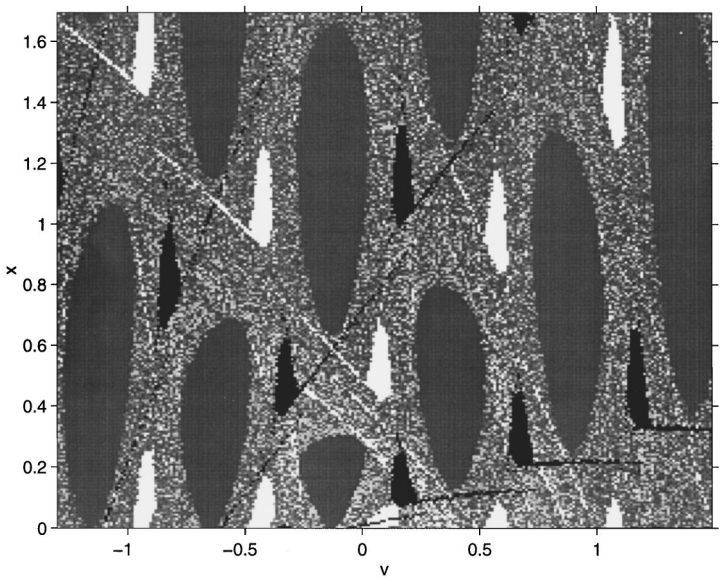

FIG. 1. Fragment of the phase space of the bouncer obtained by iterations of the stroboscopic map. Large elliptic regions represent islands of the EM, the brightest regions depict islands of the AM, and the darkest regions depict islands of the DAM ($g=1.0$, $\xi=0.75$, and $\varepsilon=1.25$).

For reasons that will become clear later, it is essential to know the dependence on n of the areas of the regular modes of the SM. Numerical simulations (see Sec. V) reveal that areas of the AM islands grow linearly with n. Since the SM preserves area this means that when v grows, trajectories from the DM are captured by these islands. Meanwhile, areas of the DAM islands linearly decrease with n, which means in turn that some trajectories are escaping from the DAM to the DM. To be exact, there is the third process that also takes place. It is the passing of trajectories from the DAM directly to the AM. Simple calculations show that the central trajectory from the DAM does not become the central trajectory in the AM. The numerical iterations reveal, however, that there exists a fiber of trajectories surrounding the central trajectory in the DAM that is captured by the AM.

The same effects of exchange of trajectories between modes is visible also in numerical treatments of the CM. Let us note that in the CM a trajectory changes modes at $t=t_n$ and remains in the same mode between collisions. This time, however, areas of all three types of islands are practically constant. This result is consistent with the previously noted dependence on n of islands in the SM. In fact, the following relations may be established for areas J of regular modes: For the mth EM, $J_m^{(e)}=\int dv\ dx=(g/2)^2\int|p_n-\varepsilon\dot{I}(t_n)/2|dp_n dt_n\simeq(g/2)^2 mS^{(e)}$. Here $S^{(e)}$ is the area of the elliptic mode in the CM and the vanishing of the integral of $\dot{I}$ over an elliptic island is assumed. In the same way one obtains the areas for the accelerator and deaccelerator modes that start from an island with $p_0\simeq N$: $J_{N+n}^{(\mathrm{acc})}=(g/2)^2(N+n)S^{(\mathrm{acc})}$ and $J_{N+n}^{(\mathrm{deacc})}=(g/2)^2(N-n)S^{(\mathrm{deacc})}$, with $S^{(\mathrm{acc})}=S^{(\mathrm{deacc})}$ the areas of appropriate islands in the CM. The numerically tested independence of $S^{(e)}$, $S^{(\mathrm{acc})}$, and $S^{(\mathrm{deacc})}$ on p_n is assumed here.

A family of m elliptic islands has the total area proportional to m^2. Consecutive islands in the AM grow linearly with n, while those in the DAM linearly decrease. In Fig. 2 the dependence of $J_n^{(\mathrm{acc})}$ on n is given for islands in the SM that correspond to $\tau=1$. In the AM or DAM of the CM, n iteration steps that start with $p_0=N$ correspond in the SM to $(2N+n-1)n/2$ or $(2N-n+1)n/2$ iterations steps, respectively. An iteration step in the SM takes place in a unit of time. Therefore the rate of increase $R_N^{(\mathrm{acc})}$ of the $J_N^{(\mathrm{acc})}$, i.e., the increase in time of areas of islands given in Fig. 2, is equal to

$$R_N^{(\mathrm{acc})}=(J_{N+1}^{(\mathrm{acc})}-J_N^{(\mathrm{acc})})/N=S^{(\mathrm{acc})}/N, \tag{6}$$

i.e., the rate decreases with increasing v. The formula for the rate of decrease of the deaccelerator islands can be written in a similar way.

To conclude this section we stress that the effects of exchanging trajectories between diffusive mode and some regular modes (AM and DAM) cannot be observed for the case of approximated maps and therefore it is a different feature in comparison to the standard map.

III. DIFFUSION EQUATION

We will use notions of probability densities to find a trajectory in a given mode. It follows from what was said above

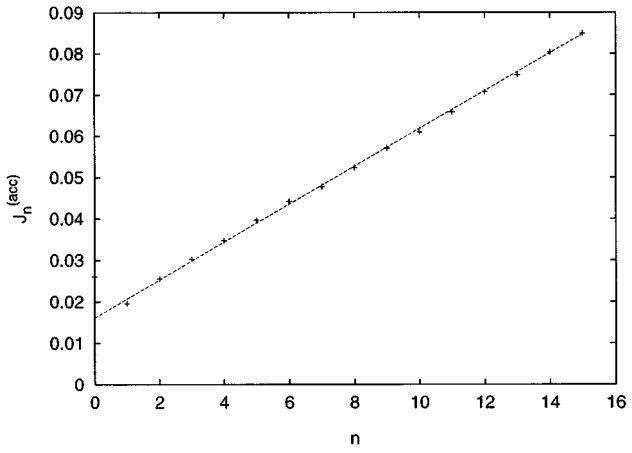

FIG. 2. Dependence of the numerically computed areas $J_n^{(\mathrm{acc})}$ of islands in the accelerator mode on values of the scaled momentum $p_n=n$. The straight line represents the least-mean-squares fit. The adopted parameters values are $g=1.0$, $\xi=0.75$, and $\varepsilon=1.25$.

that there is a flow of probability from the DM to the AM as well as from the DAM to the DM. Therefore, the DAM acts as a source for the DM, while the AM appears as a sink to the DM. The simplest way in which it can be seen how trajectories exchange modes is to run the map forward and backward. Being iterated forward, an island in the AM maintains its initial area and a compact form within new, consecutively enlarging compact islands. When iterated backward the island disperses in the sea of chaotic motions. An island in the DAM is characterized by an exactly opposite behavior. Such an interplay between modes will eventually result in the ''sucking out'' by the AM of all of the probability from outside the elliptic islands, i.e., probabilities from the DM and the DAM. Thus the AM in the bouncer has the property that is entirely different from the sticking and latent properties of accelerator modes in other maps.

The chaotic component of the bouncer dynamics, i.e., the DM, will now be described as diffusion of the action I. The diffusion coefficient can be simply derived when one assumes that in the CM the variable t_n randomizes much more rapidly than p_n. Recalling the relation between the energy E and the action I for the bouncer with $l(t)\equiv 0$: $2E=(3\pi gI/2)^{2/3}$, one gets, from the ACM, an increase of the action due to a collision with a moving plate: $(\Delta I)^2\simeq 16/\pi^2 g^2(3\pi gI/2)^{4/3}\dot{l}(t)^2$. The time elapsed between the collisions is equal to $\Delta t=(2/g)(3\pi gI/2)^{1/3}$. Since $\langle \dot{l}^2\rangle\equiv\int_0^1 \dot{l}^2(t)dt=\varepsilon^2 g^2/48$, the diffusion coefficient $D(I)=\langle(\Delta I)^2\rangle/\Delta t=D_0 I$, with $D_0=\varepsilon^2 g^2/16\pi$.

Let $P_D(I,t)$ be the density of the probability distribution of I at time t. We assume that the evolution of P_D is governed by the Fokker-Planck equation. If the norm of P_D is constant, i.e., if there is no exchange of probabilities between different modes, the following diffusion equation will be satisfied by $P_D(I,t)$:

$$\partial_t P_D=(1/2)\partial_I(D(I)\partial_I P_D). \tag{7}$$

This is a well-known Landau form of the Fokker-Planck equation for a Hamiltonian system [10] (see also [11]). The norm of P_D changes due to the flow of probability from the DM to the AM: a sinklike term in Eq. (7) should take care of this effect. The norm changes also because of the flow of probability from the DAM to the DM: a sourcelike term shall then be added to Eq. (7). Initial distributions P_D at $t=0$, which will be used later, will be of the $\delta(I-I^0)$ form. To be more specific, all points in an initial ensemble will (i) belong to the same energy shell $2E=(3\pi gI^0/2)^{2/3}$ and (ii) be located in chaotic parts of the shell. This class of initial distribution leaves only the dominant and most interesting flow of probability, namely, DM $\rightarrow$ AM. No source term is then necessary in Eq. (7). If initially there was some probability in the DAM, then in practice it would flow away from the DAM after a few iterations. Moreover, filling up of the AM will not be masked by an initial population of this accelerator mode.

The sink term is assumed to be in the form

$$S(I,t)=-\sum_{n=1}\alpha K_n^{(\mathrm{acc})}P_D(I_n^{(a)},t)\,\delta(I-I_n^{(a)}), \tag{8}$$

where $K_n^{(\mathrm{acc})}=(J_{n+1}^{(\mathrm{acc})}-J_n^{(\mathrm{acc})})/(I_{n+1}^{(a)}-I_n^{(a)})$. $I_n^{(a)}$'s are the values of I that correspond to $t_n^{(a)}$ and $p_n^{(a)}$, i.e., to the center of the AM; α is a dimensionless phenomenological parameter. $I_n^{(a)}$'s are calculated using the relations between the energy and the action introduced above. $K_n^{(\mathrm{acc})}$ is equal to this amount of the phase space captured by the AM islands in a unit of time, which corresponds to the unit growth of the action. For large n, $K_n^{(\mathrm{acc})}$ behaves like $1/n^2$. In terms describing the sink, the diffusion probability density is approximated by the δ-type distributions located at I's corresponding to centers of islands. The full equation for the P_D now has the form

$$\partial_t P_D=\partial_I[D(I)/2\partial_I P_D]+S(I,t). \tag{9}$$

In order to solve Eq. (9), the solution $P_D^{(0)}(I,I^0,t)$ of Eq. (7), which has the property $P_D^{(0)}(I,I^0,0)=\delta(I-I^0)$, will now be given.

The double Laplace transform of $P_D^{(0)}(I,I^0,t)$, namely,

$$f(s,q,I^0)=\int_0^\infty\int_0^\infty P_D(I,I^0,t)\exp(-st-qI)dt\,dI,$$

is easily found and has the form

$$f(s,q,I^0)=(1/qe^{2s/D_0q})\int_0^q 1/q'\,e^{-[2s/(D_0q')+q'I^0]}dq'. \tag{10}$$

Fortunately enough, not going beyond the standard tables of Laplace transforms, the inverse transform can be found and it reads

$$P_D^{(0)}(I,I^0,t)=(2/D_0t)\exp[-2(I+I^0)/D_0t]\times I_0(4(II^0)^{1/2}/D_0t), \tag{11}$$

where I_0 is the modified Bessel function of the first kind. $P_D^{(0)}(I,I^0,t)$ is normalized to unity for all times.

With the help of the function $P_D^{(0)}$, Eq. (9) may be transformed to the integral form

$$P_D(I,I^0,t)=P_D^{(0)}(I,I^0,t)-\alpha\sum_{n=1}K_n^{(\mathrm{acc})}\int_0^t P_D^{(0)}(I,I_n^{(a)},t-t')\times P_D(I_n^{(a)},I^0,t')dt'. \tag{12}$$

If $I=I_m^{(a)}$, $m=1,2,\ldots,L$, is substituted into Eq. (12) and the sum is limited to L terms, then we obtain a system of L coupled Volterra-type integral equations for the functions $P_D(I_n^{(a)},I^0,t)$, $n=1,2,\ldots,L$. For comparison with numerical simulations, these equations were solved for $L=12$. The set of functions $P_D(I_n^{(a)},I^0,t)$, $n=1,2,\ldots,L$, calculated in this way will suffice to determine P_D from Eq. (12) as well as P_{ACC} from Eqs. (13) and (14) (see below).

IV. PROBABILITY IN THE ACCELERATOR MODE

The density of the probability distribution in the AM is consequently written in the form

$$P_{\mathrm{ACC}}(I,t)=\sum_{n=1} P^{(n)}_{\mathrm{ACC}}(I^{(a)}_n,t)\,\delta(I-I^{(a)}_n). \tag{13}$$

For $t>0$ the flow of probability from the DM starts to populate each component of the $P_{\mathrm{ACC}}(I,t)$. It is not particularly complicated to write down the formula for $P^{(n)}_{\mathrm{ACC}}(I^{(a)}_n,t)$. It reads

$$P^{(n)}_{\mathrm{ACC}}(I^{(a)}_n,t)=\alpha K^{(\mathrm{acc})}_n\int_{[t-n]}^{t} P_D(I^{(a)}_n,I^0,t')dt' + \sum_{j=1}^{n-1}\alpha K^{(\mathrm{acc})}_j\int_{d(n,j)}^{u(n,j)} P_D(I^{(a)}_j,I^0,t')dt', \tag{14}$$

where $d(n,j)=[t-\Sigma_{i=j}^{n} i]$ and $u(n,j)=[t-\Sigma_{i=j}^{n-1} i]$. Square brackets used in the limits of the integrals have the meaning $[l]=(l+|l|)/2$.

For all values of $I^{(a)}_n$ and at any instant of time the probability from the DM is leaking to the AM. Once in the mode, the probability flows according to the dynamics characteristic to the AM, i.e., it stays for n units of time on the $I^{(a)}_n$ shell. The formula (14) properly takes care of both features.

The integration of the $P_{\mathrm{ACC}}(I,t)$ over I gives the norm

$$\int_0^\infty P_{\mathrm{ACC}}(I,t)dI=\sum_{n=1} P^{(n)}_{\mathrm{ACC}}(I^{(a)}_n,t).$$

After the rearrangement of the double sums in the above equation, it can be written as

$$\int_0^\infty P_{\mathrm{ACC}}(I,t)dI=\alpha\sum_{n=1} K^{(\mathrm{acc})}_n\int_0^t P_D(I^{(a)}_n,I^0,t')dt'. \tag{15}$$

From Eqs. (12) and (15) it follows that

$$\int_0^\infty [P_D(I,I^0,t)+P_{\mathrm{ACC}}(I,t)]dI=1,$$

i.e., the sum of probabilities in the DM and AM is properly normalized for all instants of time.

V. COMPARISON WITH NUMERICAL SIMULATIONS

The simplest way to obtain numerically the time evolution of an ensemble of trajectories of the gravitational bouncer is to solve equations of motion in the moving frame of reference, i.e., to change the variable $x\to y=x-l(t)$. Then $y>0$ and $\dot{y}\to-\dot{y}$ for $y=0$. Values of x and v for all trajectories from an ensemble were readily obtained for integer instants of time and the time dependence of island areas and of densities of points in the phase space were calculated.

In order to obtain the area $J^{(\mathrm{acc})}_n$ of the accelerator island in the phase space, a rectangular region was centered at the point $(x^{(a)}_n,v^{(a)}_n)$, i.e., the point that is calculated from Eq. (4) for $t_n=t^{(a)}_n$, $p=n$, and $\tau=1$. From this region, a 500×500 grid of points then evolved in time. The number of points that, after $(2n+k-1)k/2$ units of time, had $v\approx g(n+k)/2$ gave the desired value of $J^{(\mathrm{acc})}_n$ (in units of the adopted grid). It was found that for $k\gg1$ the result did not depend on k and that accelerator islands had a compact form. In this way the dependence given in Fig. 2 was obtained.

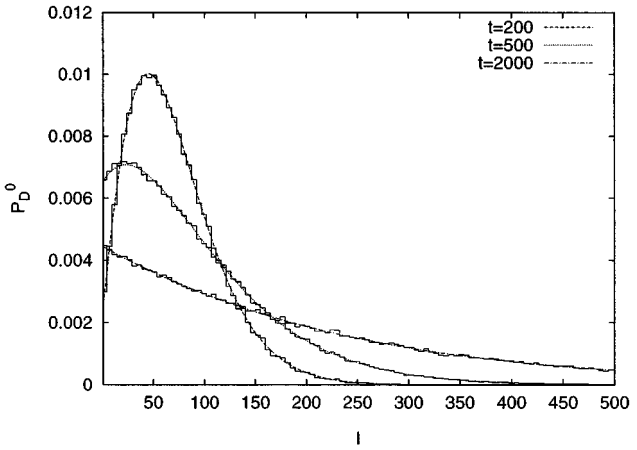

FIG. 3. Comparison of the diffusion probability density $P^0_D(I,I^0,t)$ from Eq. (11), with numerical results (histograms) for $t=100$, 500, and 2000. The values of the parameters are $g=1.0$, $\xi=0.5$, $\varepsilon=2{,}0$, $I^0=19.12$, $D_0=0.0812$.

Let us now examine formulas for the probability densities in the DM and AM. According to what was said above, we choose the initial density in the phase space in such a way that only points that belong to chaotic regions of the same energy shell are taken into account. In the first place it requires the localization and finding measures of the elliptic, accelerator, and deaccelerator regions of the considered energy shell. This means, in practice, finding arcs of the parabola $E=v^2/2+gx$, which belong to the EM, AM, and DAM islands. The uniform density of points is then assumed on the remaining portions of the parabola and these are the points that start to evolve in time. Depending on the parameters ε and ξ, the phase-space density of these points is now to be compared either with P^0_D from Eq. (11) or with P_D and P_{ACC} given in Eqs. (12) and (13).

The first choice of parameters is such that only the DM exists. The best fit with the results of numerical simulations

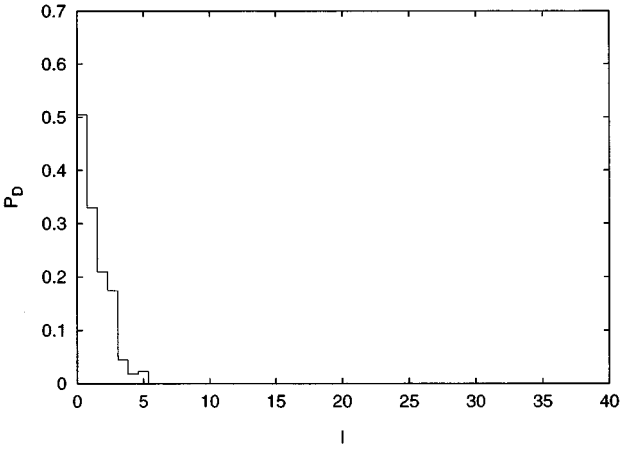

FIG. 4. Histogram of the probability density for $g=1.0$, $\xi=0.75$, $\varepsilon=1.25$, $I^0=0.61$, and $t=20$. The accelerator mode exists for these parameters.

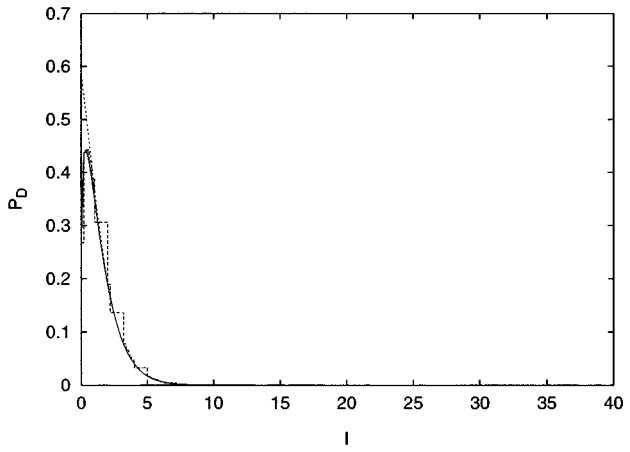

FIG. 5. Diffusion probability density $P_D(I,I^0,t)$ from Eq. (12) (solid line), diffusion probability density $P_D^{(0)}(I,I^0,t)$ from Eq. (11) (dotted line), and sum $P_D(I,I^0,t)+P_{\mathrm{ACC}}(I,t)$, with P_{ACC} from Eq. (13) being the density of the probability distribution in the AM. $D_0=0.07$ and $\alpha=1.0$. The remaining parameters and the time t are the same as in Fig. 4.

of the formula given in Eq. (11) was obtained for $D_0=0.0812$ and the comparison for several instants of time is given in Fig. 3. The rough theoretical estimation of D_0, which was presented above, gave $D_0=0.0796$ for the adopted values of parameters. Since both values of D_0 differ less than 2%, the agreement of the theory and numerical results is quite satisfactory.

Figures 4–9 present cases when the AM exists. Numerical simulations (Figs. 4, 6, and 8) are now compared with results obtained from Eqs. (12) and (13) (Figs. 5, 7, and 9). The comparison is made for $t=20$, 50, and 100. In comparison with the previous case, the existence of elliptic and accelerator islands modifies the value of the diffusion constant D_0. This time the best fit was obtained for $D_0=0.07$. The parameter α was also determined from the adjustment to the numerical data and it turned out to be $\alpha=1.0$.

In order to better visualize the escape of probability from the DM, the densities P_D (solid lines) and P_D^0 (dotted lines)

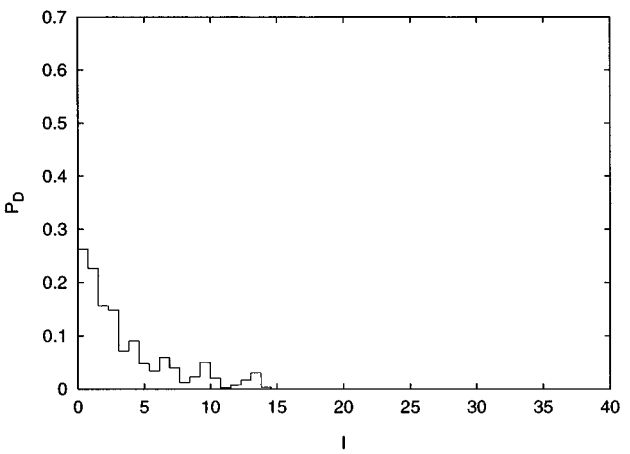

FIG. 6. Histogram of the probability density. The parameters g, ξ, and ε are the same as in Fig. 4; $t=50$.

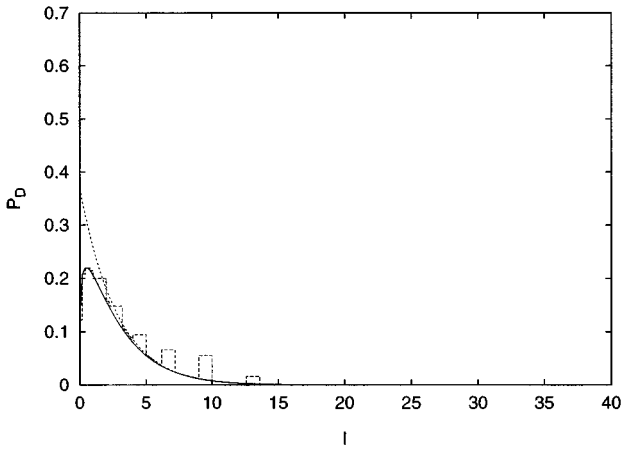

FIG. 7. Same as in Fig. 5, for $t=50$.

are simultaneously presented in Figs. 5, 7, and 9. The AM islands have some width that grows with growing n (see Figs. 4, 6, and 8). This effect cannot be described by the model presented in this paper since δ-type densities of the AM are assumed in Eq. (13). Nevertheless, in order to make qualitative comparisons of populations of the different AM islands possible, an arbitrary constant width ΔJ was assigned. The distribution P_{ACC} appears then as a sequence of ''chimneys,'' each with a height proportional to $P_{\mathrm{ACC}}^{(n)}(I_n^{(a)},t)$; see Eq. (14). The chimneys are added to the P_D distributions in Figs. 5, 7, and 9.

Contributions from the AM to histograms given in Figs. 4, 6, and 8 can be numerically evaluated at least for such values of n where the diffusion component is negligible. This has been done for the histogram in Fig. 8. In Table I the probabilities located in the AM islands in Fig. 8 are compared with probabilities $P_{\mathrm{ACC}}^{(n)}(I_n^{(a)},t)$ for $t=100$ and $11\leqslant n\leqslant 15$. It follows from the theory that after 100 units of time the sum of probabilities in all islands of the accelerator mode is equal to 0.294.

The agreement of simulations and derived formulas is certainly not as good as that in Fig. 3. From a long list of more or less obvious causes of such a state of affairs let us mention only one. These AM islands, which are mostly to the right,

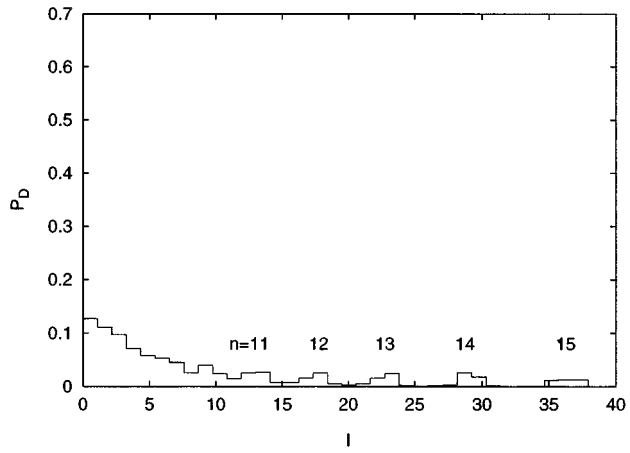

FIG. 8. Histogram of the probability density. The parameters g, ξ, and ε are the same as in Fig. 4; $t=100$.

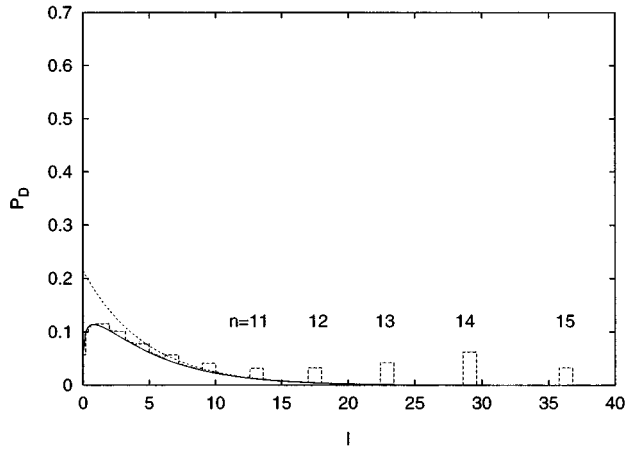

FIG. 9. Same as in Fig. 4, for $t=100$.

were populated during initial instants of time, i.e., within the time interval when not yet enough collisions had taken place and the description in terms of diffusion was questionable.

VI. SUMMARY AND CONCLUDING REMARKS

We studied conditions for the existence of the accelerator mode in the model of a gravitational bouncer, i.e., a point that bounces elastically on an oscillating plate. A parabolic approximation, with parametrically $(0<\xi<1)$ regulated contributions of convex and concave parts, was used to describe the oscillations. It was well known that for the appropriate range of parameters in the phase space of this model there were regions of resonance, periodic motions, that were embedded in the sea of the chaotic motion. We have shown that when the resonance islands existed and $\xi>0.5$, there were also two regular types of motions: the accelerator and the deaccelerator modes. It was also known that accelerator modes enhanced the diffusion in the chaotic part of the phase space. Latent or quasiaccelerator modes, as well as sticky accelerator modes, were introduced in a number of models. On a sufficiently long time scale, these modes did not change the norm of the probability density in the diffusive mode. This is not the case in the model considered in this paper. Examining maps, which describe the time evolution of the bouncer, it has been demonstrated that the probability located in the accelerator mode monotonically increased in time. In other words, the accelerator mode attracted (sucked out) the probability from the diffusive mode with the result that eventually only periodic and accelerated trajectories remained. This is the different property of accelerator modes. The above-mentioned features were quantitatively described. The exact solution of the Landau-type diffusion equation for the conditional probability density of the action I, in which the diffusion coefficient depends linearly on I, was given. The sinklike term, responsible for the presence of the accelerator mode, was then added to the diffusion equation. The solution of the full equation for the diffusive probability density was obtained via the transformation of the differential equation into a set of coupled Volterra-type integral equations. The latter was solved numerically. The density of the probability in the accelerator mode was found in such a way that the norm of the sum of both probabilities was time independent. Fairly good agreement of analytical and numerical results with ''computer experiments'' was finally demonstrated.

TABLE I. Probabilities located in islands of the accelerator mode at $t=100$. The values of the parameters are the same as in Fig. 4. $P_{\mathrm{ACC}}^{(n)}$ probabilities calculated from Eq. (14); $\mathcal{P}_{\mathrm{ACC}}^{(n)}$, probabilities evaluated from the histogram in Fig. 8.

n	$P_{\mathrm{ACC}}^{(n)}$	$\mathcal{P}_{\mathrm{ACC}}^{(n)}$
11	0.020	0.020
12	0.027	0.028
13	0.039	0.041
14	0.057	0.062
15	0.041	0.033

When oscillations of the reflecting plate are described by another periodic function of time the attracting modes with similar properties also exist in gravitational bouncers. A quantized version of the problems discussed in this paper, including in particular the effect of tunneling from the accelerated mode, will be the subject of a subsequent paper.

Let us conclude with the following remark. It seems that the properties of the accelerator mode, which we described above, are closer to Fermi's expectations of acceleration of cosmic particles than those features that follow from the model that bears his name in which there is an upper bound for the increase of energy.

ACKNOWLEDGMENT

This work has been partly supported by the Polish Government (KBN Grant No. 2P302 100 07).

[1] A. B. Rechester, M. N. Rosenbluth, and R. B. White, Phys. Rev. Lett. **44**, 1586 (1980).
[2] A. B. Rechester, M. N. Rosenbluth, and R. B. White, Phys. Rev. A **23**, 2664 (1981).
[3] B. V. Chirikov, Phys. Rep. **52**, 263 (1979).
[4] Y. H. Ichikawa, T. Kamimura, and T. Hatori, Physica D **29**, 247 (1987).
[5] C. F. F. Karney, Physica D **8**, 360 (1983).
[6] C. F. F. Karney, A. B. Rechester, and R. B. White, Physica D **4**, 425 (1982).
[7] A. J. Lichtenberg, M. A. Lieberman, and N. W. Murray, Physica D **28**, 371 (1987).
[8] J. D. Hanson, E. Ott, and T. M. Antonsen, Jr., Phys. Rev. A **29**, 819 (1984).
[9] S. T. Dembiński, A. J. Makowski, and P. Peplowski, Phys. Rev. Lett. **163**, 143 (1992).
[10] L. Landau, Zh. Eksp. Teor. Fiz. **7**, 203 (1937).
[11] A. J. Lichtenberg and M. A. Liebermann, *Regular and Chaotic Dynamics* (Springer, New York, 1992).
[12] S. Bullet, Commun. Math. Phys. **107**, 241 (1986).